Available online at www.sciencedirect.com

SciVerse ScienceDirect

Acta Materialia 60 (2012) 3741–3747

Acta MATERIALIA

www.elsevier.com/locate/actamat

Low temperature uniform plastic deformation of metallic glasses during elastic iteration

Takeshi Fujita [a], Zheng Wang [b], Yanhui Liu [a], Howard Sheng [c], Weihua Wang [b], Mingwei Chen [a,d,*]

[a] WPI Advanced Institute for Materials Research, Tohoku University, Sendai 980-8577, Japan
[b] Institute of Physics, Chinese Academy of Sciences, Beijing 100190, People's Republic of China
[c] School of Physics, Astronomy and Computational Sciences, George Mason University, Fairfax, VA 22030, USA
[d] State Key Laboratory of Metal Matrix Composites, School of Materials Science and Engineering, Shanghai Jiao Tong University, Shanghai 200030, People's Republic of China

Received 7 October 2011; received in revised form 24 February 2012; accepted 18 March 2012

Abstract

Molecular dynamics simulations and dynamic mechanical analysis experiments were employed to investigate the mechanical behavior of metallic glasses subjected to iteration deformation in a nominally elastic region. It was found that cyclic deformation leads to the formation of irreversible shear transformation zones (STZs) and a permanent uniform strain. The initiation of STZs is directly correlated with the atomic heterogeneity of the metallic glass and the accumulated permanent strain has a linear relation with the number of STZs. This study reveals a new deformation mode and offers insights into the atomic mechanisms of STZ formation and low temperature uniform plastic deformation of metallic glasses.

Keywords: Metallic glasses; Simulation; Plastic deformation

1. Introduction

It was reported a long time ago that low temperature plastic deformation of metallic glasses is solely accomplished by spatially localized shear bands [1–9]. Surprisingly, recent experimental observations suggest that uniform plastic deformation of metallic glasses can occur at room temperature when the sample size as small as hundreds of nanometers or in bulk samples subjected to long-term elastostatic compression [10–14]. Several suggestions have been proposed to explain the unusual deformation behavior, such as deformation-induced structure disorder [13,14] and atomistic free zones [15]. Since uniform plastic deformation usually requires the activation and cooperation of a large number of atoms and atomic-scale defects by either diffusion-controlled creep or rate-related viscous flow [4], both of which only take place at high temperatures, the underlying mechanisms of low temperature uniform plastic deformation of metallic glasses remain a mystery.

Limited by a low atomic mobility and kinetic energy, the stress-driven mechanical instability of metallic glasses at room temperature is usually associated with spatially heterogeneous shear transformation zones (STZs). Once the applied stress is high enough to activate a critical number of STZs that are interconnected to form an incipient zone, a localized shear band will form, leading to macroscopic yielding, plastic deformation and failure of the metallic glass [3–5]. Therefore, understanding the formation of STZs in uniformly deformed samples may provide essential clues to the atomistic mechanism of low temperature uniform plasticity of metallic glasses. In this study we employed a quantitative computational method as well as

* Corresponding author at: WPI Advanced Institute for Materials Research, Tohoku University, Sendai 980-8577, Japan.
E-mail address: mwchen@wpi-aimr.tohoku.ac.jp (M.W. Chen).

1359-6454/$36.00 © 2012 Acta Materialia Inc. Published by Elsevier Ltd. All rights reserved.
http://dx.doi.org/10.1016/j.actamat.2012.03.032

dynamic mechanical analysis (DMA) to investigate the cyclic shear deformation of a chemically heterogeneous $Cu_{45}Zr_{45}Ag_{10}$ metallic glass, which reveals the inherent correlation between structure-related STZ formation and uniform plastic deformation of metallic glasses.

2. Simulation technique and experimental details

2.1. Molecular dynamics simulations

We utilized the LAMMPS molecular dynamics (MD) package [16] to simulate cyclic shearing of a $Cu_{45}Zr_{45}Ag_{10}$ (at.%) metallic glass. The many-body potentials of the Cu–Zr–Ag system used in the calculations were developed using the embedded atom method (EAM) [17] and were optimized in our previous study [18,19] (the file with the EAM potential is available at: http://sites.google.com/a/gmu.edu/eam-potential-database/). More technical details on the optimization of EAM potentials have been described elsewhere [17,20]. MD calculations were performed in the *NPT* ensemble (i.e. a constant number of particles, constant pressure, and constant temperature, $P = 0$) with 128,000 atoms under periodic boundary conditions. The systems underwent melting at 2000 K for 0.1 ns (with a time step of 5 fs) and then were cooled from 2000 down to 100 K at a cooling rate of $\sim 2 \times 10^{11}$ and $\sim 2 \times 10^{10}$ K s^{-1}. A Nose/Hoover thermostat was applied to control the temperature. The final dimensions of the glassy samples at 100 K were $13.2 \times 13.2 \times 13.2$ nm. Mechanical shear was applied with a time step of 2 fs at a constant shearing rate ($\dot{\gamma}_{xy}$) of 10^{-3} or 10^{-5} ps^{-1} at a constant temperature of 100 K. Periodic boundary conditions were applied to the sample during the shearing process to eliminate surface effects. The applied stress was calculated from the *xy* tensor component with respect to the entire system.

2.2. Cycling tensile experiments

Glassy ribbons with the nominal composition $Cu_{45}Zr_{45}Ag_{10}$, the same as the MD simulated alloy, were prepared by a melt spinning method at a cooling rate of 10^5–10^6 K s^{-1}. The amorphous nature of the as-prepared samples was verified by XRD diffraction and transmission electron microscopy. Cyclic tensile experiments with the glassy ribbons were conducted using a dynamic mechanical analysis (DMA) system (TA Instruments Q-800) at room temperature. The maximum loading stress was ~800 MPa, which is approximately 70% of the macroscopic yield strength. The loading rate of the cycling loading and unloading was 142 MPa min^{-1} for each cycle. The test samples were characterized by scanning electron microscopy (JEOL JIB-4600F) at high magnification.

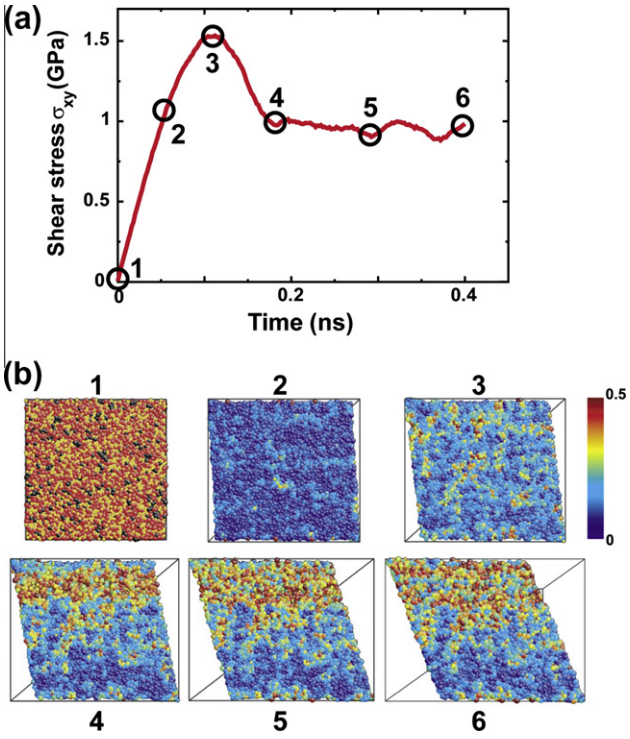

Fig. 1. (a) MD simulation of the shear stress vs. time relation of a $Cu_{45}Zr_{45}Ag_{10}$ glass with 128,000 atoms. The shear rate $\dot{\gamma}_{xy}$ is 10^{-3} ps^{-1}. (b) Atomic configurations and local shear strain maps corresponding to marked numbers in (a). The initial atomic configuration is at 1, where yellow, red, and black balls represent Cu, Zr, and Ag atoms, respectively. The local shear strain, indicated by the colored scale bar, is visualized in maps 2–6. (For interpretation of the references to color in this figure legend, the reader is referred to the web version of this article.)

3. Results

3.1. MD simulation of shear deformation

The shear stress vs. time curve of a single shear deformation from the MD simulation is shown in Fig. 1a. The stress increases monotonically, reaches the yield point and then decreases slightly for subsequent steady flow. During the shear deformation, the local shear strain $\eta^{\text{von Mises}}$, referenced to the initial atom positions prior to loading [21], was monitored. Fig. 1b shows the initial atomic configuration (point 1 in Fig. 1a), as well as $\eta^{\text{von Mises}}$ maps corresponding to points 2–6 marked in the shear stress vs. time curve. The initial atomic structure of the glass, as previously characterized [18,19], consists of a large number of interpenetrating clusters with interdigitating Ag atomic chains. In this study the Ag chains serve as internal marks to inspect the atomic processes of heterogeneous deformation. During loading in the nominal elastic regions the number of STZs with significant strain localization increases with applied stress. At the yield point (3) the accumulated STZs link together to form 1–2 nm incipient zones that eventually

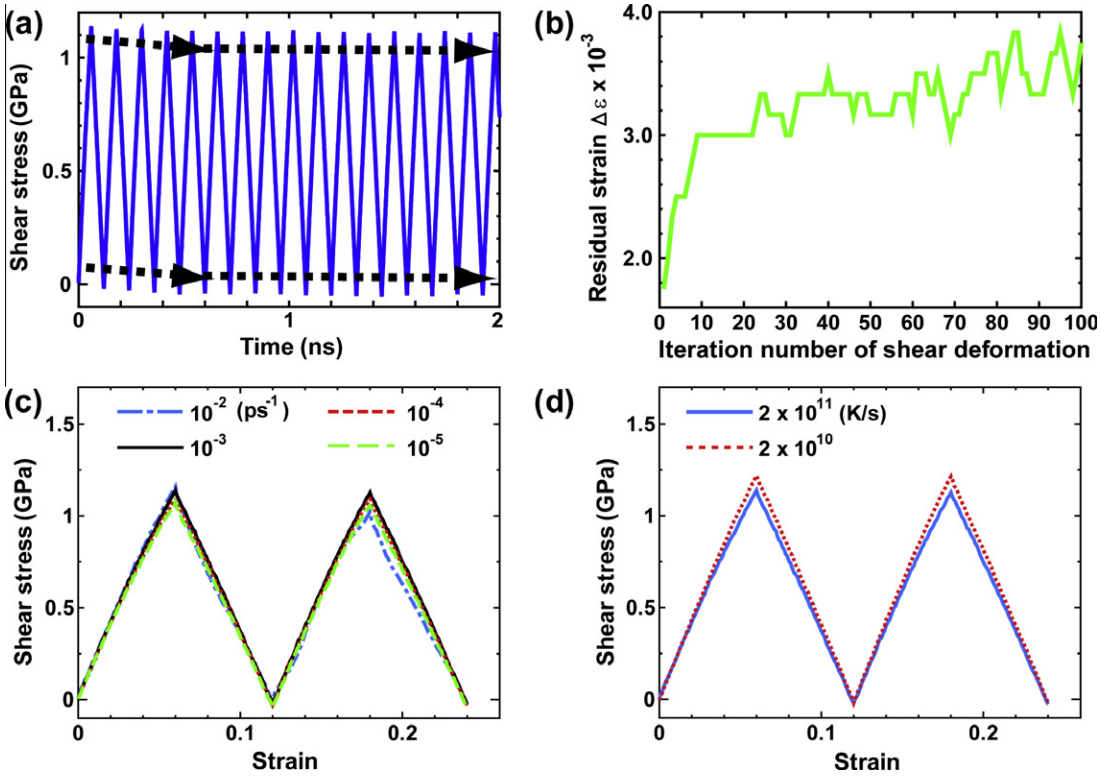

Fig. 2. MD simulation of (a) the stress–time relation of the elastic iterations (only the first 17 cycles are shown here) at $\dot{\gamma}_{xy} = 10^{-3}$ ps^{-1} and (b) a plot of residual strain $\Delta\varepsilon$ vs. iteration number. (c) Stress–imposed strain relationship for the first two cycles with different shear rates for comparison, which indicates a weak shear rate dependence. (d) Stress–imposed strain relationship for the first two cycles using two atomic configurations from the different cooling rates for comparison, which indicates a weak cooling rate dependence on initial atomic configuration. $\dot{\gamma}_{xy} = 10^{-3}$ ps^{-1}.

evolve as a single shear band during further deformation (4–6). The transition from elastic deformation to localized plastic deformation is consistent with previous MD simulations reported in the literature [22–25].

3.2. MD simulation of elastic shear iteration

In this study the focus is on the nominal elastic region prior to the macroscopic yield point to reveal the relationship between low temperature uniform plastic deformation and the evolution of inherent atomic structure using a cyclic shear deformation scheme as shown in Fig. 2a. The total shear strain is increased by shearing the sample with an applied shear stress of up to 70% of the yield strength, and then gradually returns to the initial condition with 0% shear strain. We performed a total of 100 iterations of shear deformation with a constant stress amplitude and shear rate. As the number of iterations increases both the peak and valley stress levels decrease slightly, leading to residual plastic deformation under zero stress conditions. It can be seen that an obvious decrease in stress takes place in the first five cycles, which gradually becomes insignificant, as denoted by the arrows in Fig. 2a. We estimated the residual permanent strain $\Delta\varepsilon$ at zero stress of each cycle. $\Delta\varepsilon$ is mainly produced within the first 10 iterations and then slowly increases to a maximum of $\sim 3.5 \times 10^{-3}$ (0.35%) up to 100 iterations (Fig. 2b). We also conducted a simulation at a low shear rate of 10^{-5} ps^{-1} and found that the residual plastic strain has only a weak dependence on deformation rate (Fig. 2c). Moreover, a similar residual strain was observed in the sample produced at a low cooling rate of $\sim 2 \times 10^{10}$ K s^{-1} (Fig. 2d). It is worth noting that the applied stress of 70% of the yield strength appears to be the threshold value for detectable plastic strain induced by elastic shear iteration. When the stress level is below the threshold the residual strain is too small to be detected.

3.3. DMA cycling experiments

To confirm the MD predictions for low temperature uniform deformation of metallic glasses we conducted cyclic tensile experiments on the $Cu_{45}Zr_{45}Ag_{10}$ glass with a maximum stress of ~70% of the yield strength. Fig. 3a and b shows stress vs. time and strain vs. time curves for the DMA cycling tests. At a constant stress amplitude detectable plastic deformation can be observed in the strain–time plot. Slightly differently from the MD simulation, most residual uniform plastic strain (~0.2%) was achieved in the first cycle, reaching a maximum of ~0.23% in the eighteenth cycle and then remaining nearly constant up to the two hundredth cycle. This disparity in deformation time may be due to the much slower deformation rate in the DMA experiment compared with the MD simulation. Interestingly, the experimental residual strain is comparable with the value

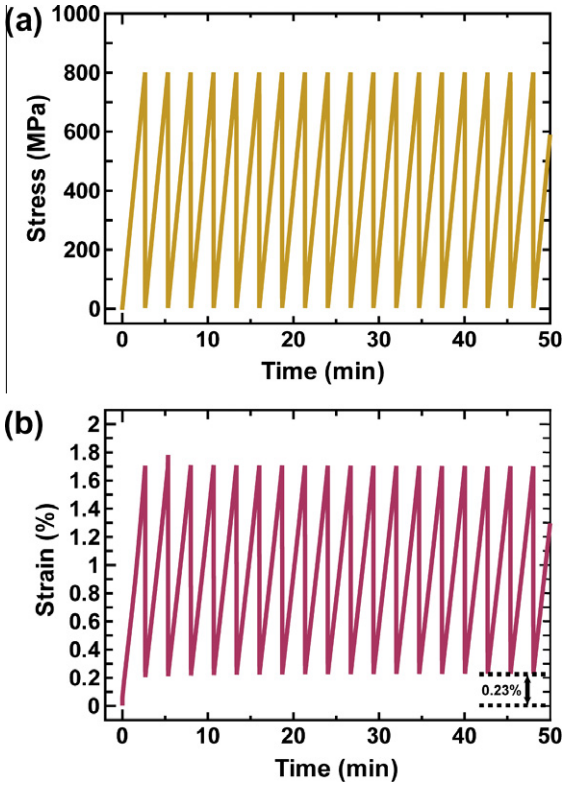

Fig. 3. DMA experiment (a) stress–time and (b) strain–time curves. In the DMA test the residual strain of ~0.2% can be observed during the first cycle, which increases up to 0.23% during the eighteenth cycle.

(0.35%) predicted by our MD simulation. The small difference may result from the differences in cooling rate, deformation rate and loading conditions (shear in the simulation and tension in the experiment). Moreover, shear bands can not be found in the tested ribbon samples on careful SEM characterization.

4. Discussion

To understand the atomic mechanisms of low temperature uniform deformation we calculated a series of $\eta^{\text{von Mises}}$ maps at the start points of each shearing cycle and monitored the evolution of the $\eta^{\text{von Mises}}$ distribution on the *xy* plane (see Supplementary movie). It can be observed that some regions with a volume of ~1 nm^3 show much higher shear strains than the matrix, and the local strain shows no change during subsequent iterations once generated, although the maximum stress is still macroscopically elastic. These regions correspond to irreversible STZs. Accompanying the shear cycling the number of STZs, defined by $\eta^{\text{von Mises}}$ values greater than a critical shear strain (0.0267) determined from a scaling analysis [26], gradually increases, with most STZs formed within the first 10 cycles (Fig. 4a). The residual strain has a linear relation with the number of STZs (Fig. 4b), indicating that uniform permanent deformation is intrinsically correlated with STZ formation. In general macroscopic plastic deformation requires long-range displacement of constituent atoms by various deformation modes, such as dislocations in crystals and shear bands in glasses. However, the local strain distribution (the inset of Fig. 4a) shows that individual STZs are isolated by the elastic matrix and long-range deformation zones characterized by the percolation or interconnection of STZs cannot be found. Therefore, the permanent deformation during shear iterations is caused by irreversible STZs, not by any long-range deformation, such as shear bands and long-range atom migration.

To explore the atomic origins of STZ formation and thereby uniform plastic deformation we investigated the correlation between local strain and the inherent atomic structure of the metallic glass. We plotted the correlation between local strain and the inherent atomic structure of Cu-centered polyhedra coordinated with Ag atoms (Fig. 4c). The fraction of full icosahedra with Voronoi index $\langle 0,0,12,0\rangle$ reduces with an increase in coordinated Ag atoms. The Ag-depleted regions have stronger shear resistance, whereas the Ag-rich regions yield larger local strains. Therefore, the heterogeneous Ag distribution intrinsically affects the formation of STZs: the Ag-rich regions with looser atomic packing [18,19] have weaker shear resistance to the initiation of STZs.

We inspected the atomic structure evolution of the samples with low applied stresses of 12–50% of the macroscopic yield strength. Even at 12% applied shear stress STZs can be observed at the first iteration. However, the total number remains nearly constant during the iteration experiments (Fig. 5a). The small number of STZs in those samples can only give rise to very limited residual plastic strain. The structural propensity for the formation of STZs at low stress levels was investigated in the same way as shown in Fig. 4c. The correlation between local strain and inherent atomic structure is actually the same as at high stress levels (Fig. 5b). This result further suggests that the STZs have a certain critical threshold point arising from the characteristics of local atomic structure in the potential energy landscape.

In our MD simulations the loading rate is much larger than that in the DMA experiments because of the inherent limitations of computational models. Therefore, the difference in plastic strain between the simulation and experiment, as shown in Figs. 2b and 3b, mainly arises from the different timescales. The fast MD loading requires more cycles to accumulate a comparable strain to that achieved in the slow DMA experiment. However, the maximum residual plastic strain appears to solely depend on the applied stress. The similar values of residual strain (0.23% for MD and 0.35% for DMA) indicate that the underlying mechanisms of plastic deformation should be the same. Moreover, the residual plastic strain achieved by elastic iteration in this study is comparable with those values reported in static experiments at similar stress levels [13,14], indicating that the micromechanisms revealed by this study may be common for all elastic deformation-induced residual plasticity in metallic glasses, including elastostatic compression [27].

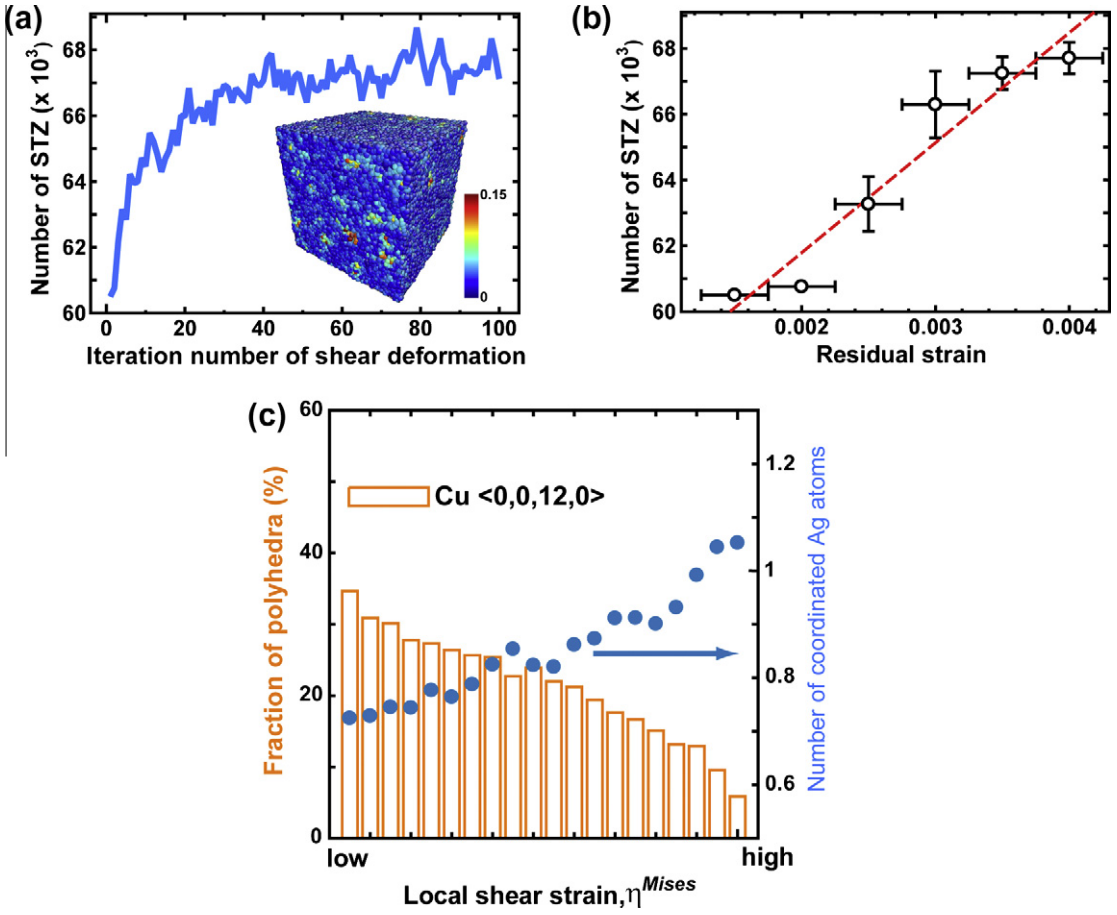

Fig. 4. (a) A plot of STZ number vs. the number of iteration cycles. (Inset) Three-dimensional map of $\eta^{\text{von Mise}}$ after the one hundredth iteration. The local strain is indicated using the colored scale bar. (b) The relation between STZ number and residual strain. The dotted line represents a least squares fitting. (c) A local strain diagram of Cu atoms after the one hundredth iteration. The fraction of the icosahedral cluster and the average number of coordinated Ag atoms for Cu atoms are counted in 20 groups with different stains. (For interpretation of the references to color in this figure legend, the reader is referred to the web version of this article.)

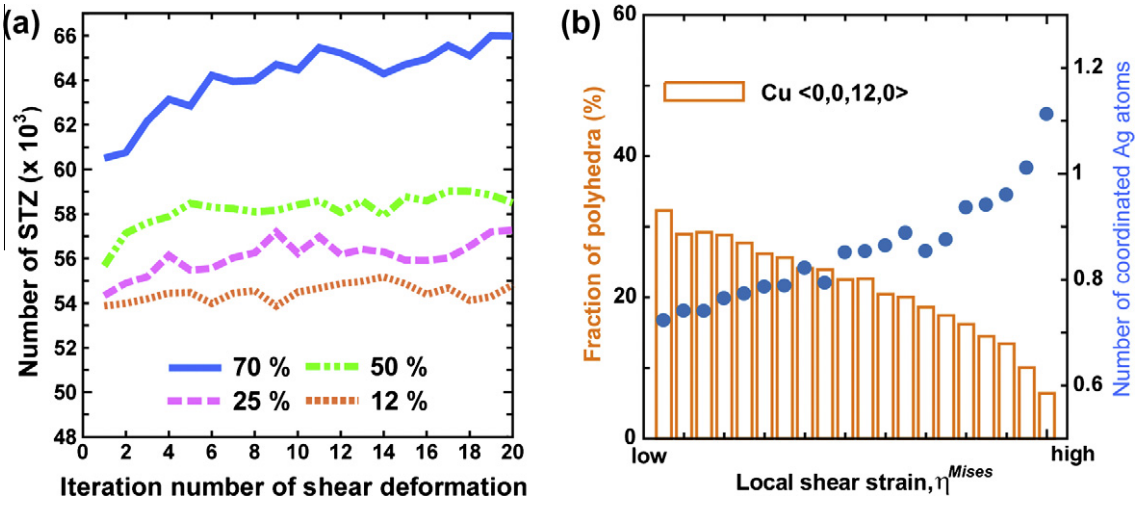

Fig. 5. (a) A plot of STZ number vs. the number of iteration cycles with different percentages of applied stress relative to the macroscopic yielding stress. (b) A local strain diagram of the Cu atoms after the twentieth iteration of 12% applied stress. The fraction of the icosahedral cluster and the average number of coordinated Ag atoms for the Cu atoms are counted in 20 groups with different stains.

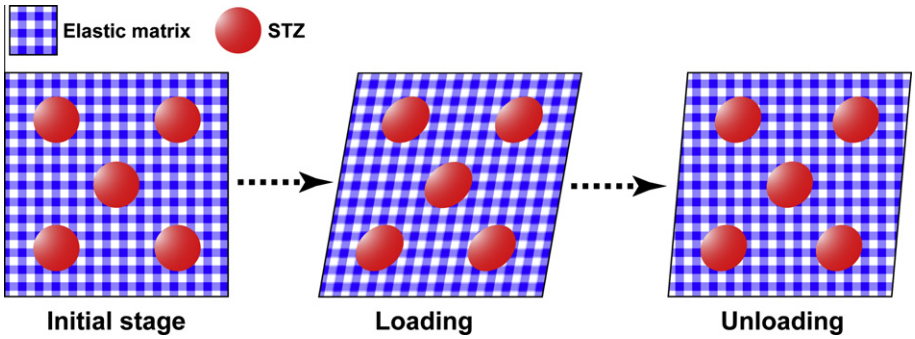

Fig. 6. Schematic illustration of the uniform deformation process. Before deformation the glassy body comprises an elastic matrix and soft STZ sites. After elastic loading the shape of the STZs with local permanent strain becomes irreversible. The summing of all local strains from the STZs gives the total uniform deformation.

In general the plastic deformation of metallic glasses at temperatures far below the glass transition point is due to multiple shear bands [28–30]. However, shear banding requires the percolation or interconnection of STZs [21], which was not seen in this study. Based on the atomic scale analysis, we outline the deformation process in Fig. 6. The glassy body consists of an elastic matrix and defective packed domains where the constituent atoms have lower coordination numbers [31–34]. During elastic loading both the elastic matrix and defective packed domains follow the shape change. However, due to the relatively low resistance of the defective packed domains to shear deformation, they may deform plastically on passing a certain critical threshold point in the potential energy landscape and become irreversible STZs. During unloading the elastic matrix tends to revert to the initial state, whereas the irreversible STZs cannot fully recover their original shape, leading to residual elastic stress and strain around the STZs. With the increase in the number of STZs and the volume fraction the local elastic strain can spread through the entire sample, resulting in overall plastic deformation. Since the accumulated plastic strain essentially originates from STZs, more STZs activated by high stresses and long-term deformation give rise to a larger plastic strain. Since the activation of STZs essentially depends on the stress, the applied stresses are the dominant factor in plasticity, while the cycling/deformation time assists the thermally activated process of STZ formation. It is interesting to note that this kind of uniform plastic deformation does not involve any long-range atomic migration and diffusion. Therefore, the MD simulation and DMA experiment in this study suggest a novel homogeneous deformation mode.

5. Summary

In this study we employed MD simulations and DMA to theoretically and experimentally investigate the low temperature uniform deformation of a bulk metallic glass subjected to nominal elastic loading. The key results are summarized below.

1. Detectable plastic deformation of the bulk metallic glass can be experimentally and theoretically achieved at low temperatures by cyclic loading with a maximum stress well below the macroscopic yield strength. Importantly, no shear bands could be observed by either MD simulation or SEM characterization, verifying that low temperature plastic strain is accomplished by a uniform deformation model.
2. Atomic scale characterization by MD simulation reveals that STZs with much larger local shear strains than the matrix can be formed at applied stresses much lower than the macroscopic yield strength. These STZs are irreversible during subsequent cyclic loading once they are generated. There is strong coupling of the STZs with the structural and dynamic heterogeneity of the bulk metallic glass. Relatively looser packing regions with greater atomic mobility have a lower resistance to the formation of STZs.
3. Uniform permanent deformation at low temperature is intrinsically correlated with the STZs. The residual plastic strain resulting from the irreversible local strain has a linear relationship with the number of STZs.
4. The MD simulation and DMA experiment in this study reveal a homogeneous deformation mode. Our novel deformation model may aid in understanding the low temperature uniform deformation that has been widely observed in elastostatic compression experiments.

Acknowledgements

This work was sponsored by the “Global COE for Materials Research and Education”, “World Premier International (WPI) Research Center Initiative for Atoms, Molecules and Materials”, MEXT, Japan. We thank the Center for Computational Materials Science, Institute for

Materials Research, Tohoku University, for affording time on the Hitachi SR11000 (model K2) supercomputing system. HWS acknowledges support from US NSF under Grant No. DMR-0907325.

Appendix A. Supplementary material

Supplementary data associated with this article can be found, in the online version, at http://dx.doi.org/10.1016/j.actamat.2012.03.032.

References

[1] Spaepen F. Acta Metall 1977;25:407.
[2] Chen HS. Mater Sci Eng 1974;13:181.
[3] Chen MW. Annu Rev Mater Res 2008;38:445.
[4] Schuh CA, Hufnagel TC, Ramamurty U. Acta Mater 2007;55:4067.
[5] Argon AS. Acta Metall 1979;27:47.
[6] Hufnagel TC, Ott RT, Almer J. Phys Rev B 2006;73:064204.
[7] Hufnagel TC, El-Deiry P, Vinci RP. Scripta Mater 2000;43:1071.
[8] Lewandowski JJ, Greer A. Nat Mater 2006;5:15.
[9] Liu CT, Heatherly L, Easton DS, Carmichael CA, Schneibel JH, Chen CH, et al. Metall Mater Trans A 1998;29:1811.
[10] Guo H, Yan PF, Wang YB, Tan J, Zhang ZF, Sui ML, et al. Nat Mater 2007;6:735.
[11] Jang DC, Greer JR. Nat Mater 2010;9:215.
[12] Volkert CA, Donohue A, Spaepen F. J Appl Phys 2008;103:083539.
[13] Park KW, Lee CM, Lee MR, Fleury E, Falk ML, Lee JC. Appl Phys Lett 2009;94:021907.
[14] Ke HB, Wen P, Peng HL, Wang WH, Greer AL. Scripta Mater 2011;64:966.
[15] Ye JC, Lu J, Liu CT, Wang Q, Yang Y. Nat Mater 2010;9:619.
[16] Plimpton SJ. J Comput Phys 1995;117:1.
[17] Cheng YQ, Ma E, Sheng HW. Phys Rev Lett 2009;102:245501.
[18] Fujita T, Konno K, Zhang W, Kumar V, Matsuura M, Inoue A, et al. Phys Rev Lett 2009;103:075502.
[19] Fujita T, Guan PF, Sheng HW, Inoue A, Sakurai T, Chen MW. Phys Rev B 2010;81:140204.
[20] Sheng HW, Kramer MJ, Cadien A, Fujita T, Chen MW. Phys Rev B 2011;83:134118.
[21] Shimizu F, Ogata S, Li J. Mater Trans 2007;48:2923.
[22] Cheng YQ, Cao AJ, Sheng HW, Ma E. Acta Mater 2008;56:5263.
[23] Shi YF, Katz MB, Li H, Falk ML. Phys Rev Lett 2007;98:185505.
[24] Li QK, Li M. Appl Phys Lett 2006;88:241903.
[25] Guan PF, Chen MW, Egami T. Phys Rev Lett 2010;104:205701.
[26] Johnson WL, Samwer K. Phys Rev Lett 2005;95:195501.
[27] Cameron KK, Dauskardt RH. Scripta Mater 2006;54:349.
[28] Schroers J, Johnson WL. Phys Rev Lett 2004;93:255506.
[29] Liu YH, Liu CT, Gali A, Inoue A, Chen MW. Intermetallics 2010;18:1455.
[30] Inoue A, Zhang W, Tsurui T, Yavari AR, Greer AL. Philos Mag Lett 2005;85:221.
[31] Liu YH, Wang D, Nakajima K, Zhang W, Hirata A, Nishi T, et al. Phys Rev Lett 2011;106:125504.
[32] Dmowski W, Iwashita T, Chuang CP, Almer J, Egami T. Phys Rev Lett 2010;105:205502.
[33] Argon AS, Demkowicz MJ. Metall Mater Trans A 2008;39A:1762.
[34] Ichitsubo T, Matsubara E, Yamamoto T, Chen HS, Nishiyama N, Saida J, et al. Phys Rev Lett 2005;95:245501.